

**Photoelectron diffraction studies of Cu on Pd(111) random surface alloys**A. de Siervo,<sup>1,2,\*</sup> E. A. Soares,<sup>3</sup> R. Landers,<sup>1,2</sup> and G. G. Kleiman<sup>1</sup><sup>1</sup>*Instituto de Física “Gleb Wataghin,” Universidade Estadual de Campinas, Caixa Postal 6165, 13081-970, Campinas, Sao Paulo, Brazil*<sup>2</sup>*Laboratório Nacional de Luz Síncrotron, Caixa Postal 6192, 13084-971, Campinas Sao Paulo, Brazil*<sup>3</sup>*Departamento de Física, Universidade Federal de Minas Gerais, Caixa Postal 702, 30123-970 Belo Horizonte, Minas Gerais, Brazil*

(Received 25 August 2004; revised manuscript received 29 November 2004; published 17 March 2005)

The study of surface alloys is motivated by their use in many applications of different segments of industry, such as in the search for new catalysts and sensors, in surface protection against corrosion, in lowering friction, and in testing electronic devices. An important aspect of surface alloys studies is that of the precise quantification of segregation and diffusion processes as well as the determination of surface structure. In this paper we report a combined low-energy electron diffraction and photoelectron diffraction (PED) (using synchrotron radiation) study of surface alloy formation when Cu ultrathin films are evaporated onto Pd(111) single-crystal surfaces. We present results for two different coverages (1 and 3 ML) and three annealing temperatures (300, 600, and 800 K). For these preparation conditions, a random alloy phase with different concentrations seems to form in the first few layers. Through the analysis of PED data performed using a multiple scattering formalism and the average  $T$ -matrix approximation it was possible to determine the atomic structure and the atomic concentration of the first three layers.

DOI: 10.1103/PhysRevB.71.115417

PACS number(s): 68.37.Ps, 61.14.Qp, 61.14.Hg, 74.70.Ad

**I. INTRODUCTION**

Over the years, many studies on epitaxial growth of thin films and surface alloy formation have been stimulated by the possibility of fabricating ultrathin metallic films with crystal phases not encountered under normal conditions, and of modifying and ultimately controlling the magnetic, electronic, and catalytic properties of the surface by lattice expansion/contraction, surface reconstruction, and alloy formation.<sup>1</sup> In applications such as that of heterogeneous catalysis, where the electronic structure, element concentrations, and geometric arrangement of the surface atoms are important, the perspective of fabricating surface alloy catalysts according to predetermined specifications for a reaction of interest is compelling.<sup>2</sup> At the present time, however, we are far from attaining such a goal. A prerequisite to understanding a catalytic reaction is the complete characterization of the surface of the catalytic agent for which it will be necessary understand the mechanisms involved in surface alloy formation.

When one metal is deposited on a single crystal face of another, one observes a number of different phenomena. The film growth mode (e.g., through island formation and layer-by-layer growth) depends on the thermodynamic characteristics of the surface-adsorbate system (e.g., surface energy) and on the kinetic characteristics of the deposition such as the evaporation rate and the substrate temperature. Also, the deposited metal could alloy with the metal substrate, which could induce surface segregation and diffusion as well as the formation of either ordered or random alloy phases.

The PdCu alloy system, which has important catalytic properties, has been the subject of many experimental and theoretical studies involving the bulk phase,<sup>3,4</sup> and different single-crystal surfaces, especially in studies of surface alloys.<sup>5-23</sup> Nevertheless, some questions remain concerning alloy formation upon Cu deposition on the Pd(111) surface.

Recently, various studies on PdCu surface alloys have appeared in the literature.<sup>5-23</sup> These studies usually involve a Pd or Cu crystal substrate cut along one of the low index planes upon whose surface Cu or Pd films are deposited in different quantities and at different substrate temperatures. The different planes present different growth and alloy formation behavior. For example, for Pd on the Cu(100) (Ref. 14) and Cu(110) (Ref. 15) faces, the growth mode is expected, from energetic arguments and confirmed by experiments, to be Volmer-Weber (VW) or island growth, and the surface presents ordered alloy phases.<sup>14,15</sup> On the other hand, for Pd on Cu(111) (Ref. 16) the growth mode is more complicated than that of a simple layer-by-layer or island growth process. The system exhibits surface alloy formation with stress relaxation through surface alloying.<sup>16</sup> Also, for approximately 1.0 ML of Pd on Cu(111), the surface alloy presents only a random phase with Pd diffusion up to the third layer after annealing at 600 K.<sup>13</sup>

For the complementary system of Cu on Pd single-crystal surfaces, which is the object of this study, the literature indicates that, despite the rather large structural misfit of 7% between the Cu and Pd lattice parameters, Cu grows layer-by-layer for Cu/Pd(100),<sup>17</sup> Cu/Pd(110),<sup>18</sup> and Cu/Pd(111).<sup>19,20</sup> However, from the points of view of alloy formation, atomic structure determination, and quantification of the surface segregation and diffusion, there are only a small number of studies, mostly theoretical, in the literature.<sup>6,7,11</sup> For Cu/Pd(111), an XPS study<sup>10</sup> correlates chemical shifts for the Cu and Pd core levels with the growth process, cluster and alloying formation, all of which depend on the annealing temperature. But, in this study,<sup>10</sup> it was not possible either to determine the atomic structure of the surface or to quantify the Cu diffusion and Pd segregation. Since PdCu surface alloys present important properties for some catalytic reactions, the precise determination of the po-

sitions and concentration of the atoms in the first few layers are crucial to understanding the physical and chemical mechanism that promote catalysis in this case.

Photoelectron diffraction (PED), which is element and surface sensitive, is ideally suited to this kind of study because of its ability to determine the relative positions of atoms and their individual concentrations in the first few layers. To our knowledge, no PED study of this surface has been reported.

In this paper, we report the application of PED in combination with low-energy electron diffraction (LEED) for the structure determination of ultrathin Cu films ( $\sim 1$  and  $\sim 3$  ML) evaporated onto a Pd(111) single-crystal surface at room temperature. The electronic structure and the Cu diffusion into Pd bulk are probed as a function of the Pd coverage and annealing temperature.

## II. EXPERIMENTAL METHODS AND DATA ANALYSIS

The experiments were performed using a bending magnet beam line and spherical grating monochromator (SGM) at the Brazilian Synchrotron Radiation Laboratory (LNLS) and a surface science workstation equipped with: LEED optics, a fixed geometry high-resolution hemispherical electron analyzer (Omicron HA125HR with multi-detection) mounted in the plane of the storage electron ring, a differentially pumped argon ion sputter gun for *in situ* sample cleaning and a two axis ( $\theta, \phi$ ) sample manipulator equipped for heating the sample to 1300 K by electron bombardment. A base pressure lower than  $2 \times 10^{-10}$  Torr was maintained in the chamber during the experiment. For collection of the PED angular scans, the sample was rotated through the polar ( $\theta$ ) and azimuth ( $\phi$ ) angles.

The substrate for the Cu ultrathin films was an electropolished 10 mm diameter Pd (111) crystal mounted on a thick Ta foil support that could be precisely aligned by three set-screws. The sample could be heated either by directly irradiating the backside of the crystal (for low temperatures) or by electron bombardment (for high temperatures). To protect the crystal from deformation, a Pd phantom of exactly the same dimensions as the crystal with a Alumel/Cromel thermocouple spot welded to its edge was used to measure a calibration curve (applied power  $x$  temperature) in order to determine the sample temperature during annealing.

Argon ion bombardment (1 kV accelerating potential and  $2.0 \mu\text{A}/\text{cm}^2$  current density on sample) and subsequent annealing up to approximately 1100 K for 5 min was used for sample cleaning. The process was repeated until no impurities could be observed with XPS using  $\text{AlK}_\alpha$  radiation. After cleaning, the sample was annealed to get a sharp LEED pattern. The LEED pattern allowed us to check the crystallinity, and also to determine precisely the initial azimuthal angle, so that the PED azimuthal angular scans always started from exactly the same orientation relative to the analyzer.

High-purity Cu (99.999%) was deposited at room temperature at 0.1 ML/min from a Mo crucible heated by electron bombardment. The Cu source was extensively degassed before use. The pressure in the chamber during the film growth was always below  $8 \times 10^{-10}$  Torr. After growing each

film, XPS analysis indicated no contaminants such as N, C, O, or S.

Cu on Pd(111) grows layer-by-layer.<sup>10,19,20</sup> The evaporation rate was calibrated by using the ratio between Cu 3*p* and Pd 3*d* XPS peak areas as a function of the evaporation time, and by observing the periodic change in the slope of the curve.<sup>10,20</sup>

The PED data was measured in the angular mode. The azimuthal angle ( $\phi$ ), was varied in steps of  $3^\circ$  over a range of almost  $150^\circ$ . Since the LEED patterns for all structures showed threefold symmetry, this range was adequate to guarantee that we measured all the structures, and replication of the data set could be used to obtain  $360^\circ$  azimuthal scans. The polar angle ( $\theta$ ), defined by the analyzer axis and the normal to the surface, was varied in  $5^\circ$  steps from  $20^\circ$  to  $60^\circ$  in most cases. The analyzer's axis subtended an angle of  $60^\circ$  relative to the propagation direction of the linear polarized photon beam, so that the electrical polarization vector was at  $30^\circ$  to the analyzer axis. The samples were excited with photons with energies in the range of 530 to 700 eV, which was high enough to ensure a good degree of forward focusing for Cu 3*p* photoelectrons and little multiple scattering for Pd 3*d* photoelectrons. A 90% transmission Au grid monitored the intensity of the radiation and the data was normalized appropriately. After each full angular scan, we verified the absence of contaminants with XPS. The method used in the data normalization was not able to eliminate completely some artifacts inherent to the measuring procedure, most probably correlated with the precession of the axis of azimuthal rotation relative to the analyzer during the sample movement. These artifacts appear in the experimental patterns as stripes with threefold symmetry due the replication process.

We used a modified version of the MSCD package<sup>21</sup> that is able to treat ordered and random alloy phases to analyze the data. The method used to describe random alloy phases is based on the average *T*-matrix approximation (ATA) (Ref. 22) and was successfully applied to Pd/Cu(111).<sup>13</sup> In this model each lattice site is occupied by an atom whose atomic scattering amplitude is equal a weighted combination of the atomic scattering amplitude of each element in the alloy.

To compare experiment and theory, normalized PED intensities  $\chi$  (Refs. 13 and 21) were used and the degree of agreement was quantified by considering the reliability factors  $R_a$  and  $R_b$ .<sup>13,21</sup> Small values of  $R_a$  and  $R_b$ , indicate good agreement between simulations and experiment.

We used a parabolic cluster type model with a radius of 11.5 Å and a depth of 12 Å with typically 280 atoms distributed in six layers. The parabolic format of the cluster, the number of atoms, the number of layers, and distribution of emitter in the layers was chosen to minimize boundary effects.

## III. RESULTS AND DISCUSSIONS

### A. The Pd (111) surface

We found no literature reports of PED studies of Pd(111), despite the importance of this surface. Since LEED (Ref. 23) and high-energy ion scattering (HEIS) (Ref. 24) studies of Pd(111) present different results, a PED determination of the

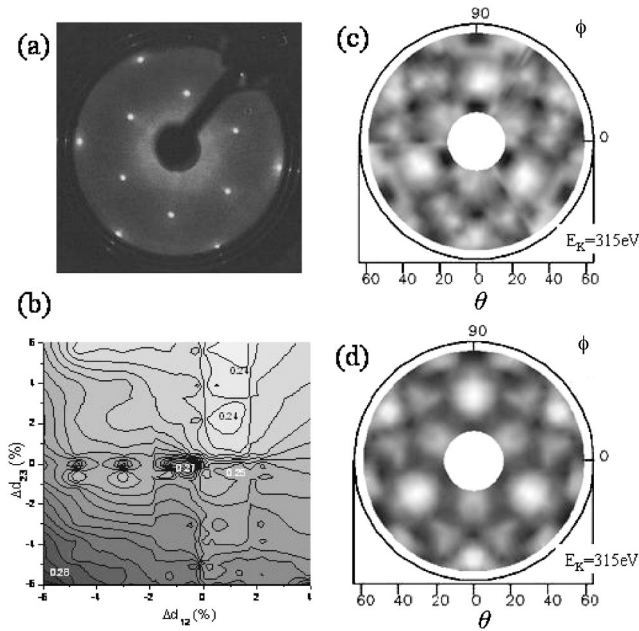


FIG. 1. LEED and photoelectron diffraction analysis for a clean Pd(111) surface. (a) LEED pattern for normally incident primary electrons of 162 eV energy. (b) Contour map of PED  $R_a$  factor analysis for Pd 3d emission as function of first and second interlayer distances related to the bulk value. (c) PED experimental raw data excited with 650 eV photons from Pd 3d, and (d) PED theoretical simulation using optimized parameters (details in the text).

interatomic distances is indicated. In Fig. 1(a) we show a very sharp LEED pattern for the clean  $p(1 \times 1)$  surface of Pd(111). The PED experiment was performed using  $h\nu = 650$  eV, yielding Pd  $3d_{5/2}$  photoelectrons with 315 eV kinetic energy, so that the photoelectrons produced are in an intermediate regime between pure forward and multiple scattering. In Figs. 1(c) and 1(d) we show, respectively, the PED raw data and theoretical simulation. Maintaining the structural parameters identical to the bulk and using a grid search procedure we first determine the inner potential and surface Debye temperature which were found to be  $9.0 \pm 2.0$  eV and  $170 \pm 15$  K, respectively. The value found for the surface Debye temperature through our comparison of theory and experiment is in good agreement with the expected value of  $\sqrt{2}/2$  of the bulk value. For the in-plane lattice parameter, we found the same value as that for bulk Pd (2.75 Å), which is expected for a closed packed surface. For the first interlayer distance we found a minimum in the  $R$  factor parameter ( $R_a = 0.24 \pm 0.1$ ) corresponding to an expansion of  $+1.2 \pm 0.5\%$  with respect to that of the bulk (2.25 Å) as is indicated in the  $R$ -factor contour map of the figure 1(b). However, for the second interlayer distance the  $R$  factor analysis was not conclusive showing different local minima. The result for the first interlayer distance is in agreement with a previous LEED study<sup>23</sup> which found an expansion of  $+1.3\%$  for the first interlayer distance and contraction of  $-1.3\%$  for the second interlayer distance. The value for the first interlayer distance also agrees with *ab initio* calculations reported by Konvicka *et al.*<sup>25</sup> The theoretical results indicate an expansion of 0.5% and a contraction of  $-0.5\%$  in the first

and second interlayer distances, respectively. However, HEIS experiments by Kuk and co-authors<sup>24</sup> indicate different results for these interlayer distances. Since the surface relaxation we found is small and because of our inability to verify the second interlayer distance, the differing HEIS results might be a product either of different experimental conditions or of different assumptions in the analysis, such the assumption of bulk termination of Pd(111).<sup>24</sup>

### B. One ML of Cu on Pd(111) as evaporated at 300 K

Reflection high-energy electron diffraction (RHEED) (Ref. 16) and scanning tunneling microscopy<sup>12</sup> (STM) studies of Pd grown on Cu(111) show a complicated behavior, with alloying in the submonolayer regime even with a substrate temperature as low as 300 K. With 1 ML of Pd evaporated on Cu(111) and annealed at 600 K, PED (Ref. 13) and theoretical<sup>26</sup> investigations indicate that Pd diffuses into the bulk of Cu(111) until at least the third monolayer with an oscillatory behavior of the Pd concentration in the first three layers. In the present study of Cu on Pd(111), we also study different coverages and annealing temperatures. In this section, we study 1 ML of Cu evaporated at 300 K.

RHEED (Ref. 20) and XPS (Ref. 10) results indicate that Cu grows layer-by-layer on Pd(111) under these conditions and does not alloy with the Pd(111) substrate. In contrast with the LEED pattern for the clean surface, that for Cu/Pd(111) is diffuse, with the same  $p(1 \times 1)$  symmetry. In order to investigate the short range order, we measured PED patterns for this surface using the Pd  $3d_{5/2}$  and Cu  $3p$  photoelectron excited with photons of  $h\nu = 530$  eV. In Fig. 2, we present both experimental PED patterns. We observe a PED pattern for the Pd 3d emitters [Fig. 2(a)] that agrees fairly well with that of the substrate. For Cu 3p emitters, however, the PED pattern does not manifest well-defined structures, in contrast with what would be expected for a highly ordered fcc film. Moreover, the bright spots for polar angles around  $35^\circ$  are slightly elongated in the azimuthal direction. This could be due to the existence of very slightly misaligned bidimensional islands that could not be identified in the diffuse LEED pattern or even in the RHEED study.<sup>20</sup> A careful STM investigation is indicated in order to determine the correct surface morphology.

Due to the diffuse nature of the Cu signal no attempt was made to exactly determine its structure. It was possible, though, to get some idea of diffusion and segregation by supposing that, in this case, a random alloy is formed in the first monolayers (as is consistent with the observed LEED pattern) and then by optimizing the “ $R$  factors” through variation of the concentrations in these layers. Since PED is sensitive to short-range order, this procedure is probably valid as a first approximation. Considering both data sets (both the Pd and Cu emitters), the best result found in our simulations indicates that Cu remains only in the first layer. This result confirms the conclusions of the XPS (Ref. 10) and RHEED (Ref. 20) studies.

### C. One ML of Cu on Pd(111) annealed at 600 K

After collecting the PED data for the 1 ML film of Cu on Pd at 300 K, the film was annealed by ramping the tempera-

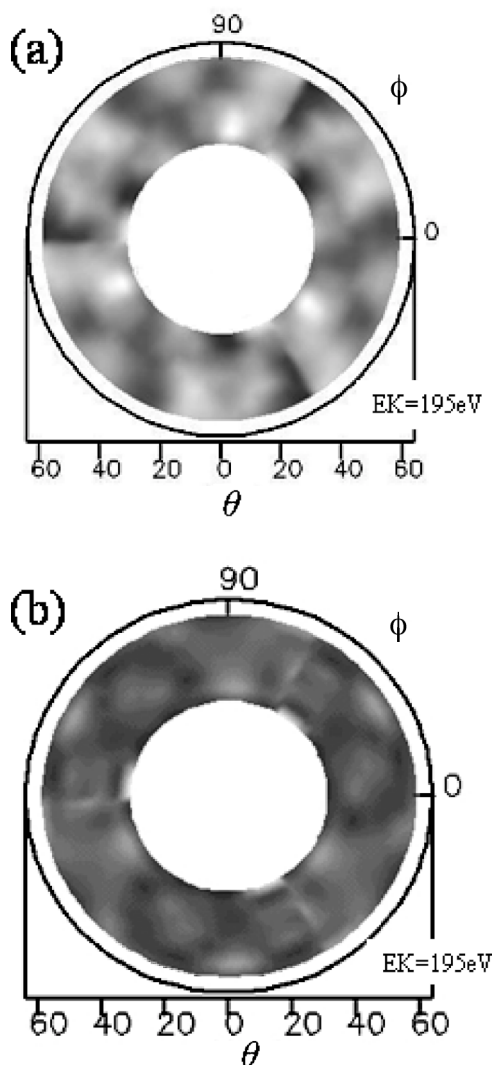


FIG. 2. Planar projection of PED patterns (raw experimental data) for 1 ML of Cu on Pd(111) surface evaporated and measured at room temperature. (a) Pd 3d emission and (b) Cu 3p emission excited with 530 eV photons.

ture from 300 to 600 K at a rate of 30 K/min and keeping the sample at 600 K for 10 min. During the annealing process, XPS spectra were periodically taken. From the Cu 3p chemical shifts, it is probable that alloy formation starts only at temperatures around 450 K, in agreement with the results of Liu, St. Clair, and Goodman.<sup>10</sup> After the annealing, a  $p(1 \times 1)$  LEED pattern, very similar to that of clean Pd(111), was observed, with a slightly higher diffuse background and without any evidence of superstructures. This behavior was similar to that for 1 ML of Pd on Cu(111) after the same annealing process.<sup>13</sup> In order to determine the atomic structure and Cu concentration in the first three layers, we used the same method described in Ref. 13 to simulate the PED experiment with the ATA approach in order to include random alloy cases.

Figures 3(a) and 3(b) present the PED raw data for Pd 3d and Cu 3p excited with  $h\nu=530$  eV photons. There are three models that are consistent with the  $p(1 \times 1)$  LEED pattern: a Cu overlayer, a Pd capping layer, and a random alloy. All

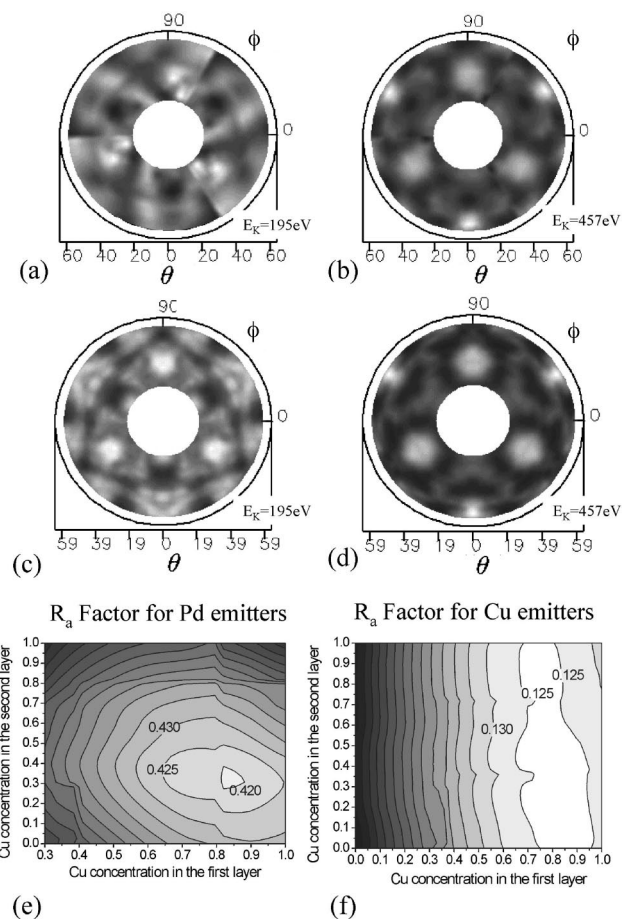


FIG. 3. Layer-by-layer determination of the surface alloy concentration and theory-experiment comparisons for PED data sets for 1 ML of Cu on Pd(111) annealed at 600 K and excited with photons of 530 eV. (a) Experimental raw data for Pd 3d emission; (b) experimental raw data for Cu 3p emission; (c) and (d) correspond to optimized PED theoretical simulations respectively for Pd 3d emission and Cu 3p emission considering a PdCu random alloy in the first and second layers with the concentrations found by the  $R_a$  factor contour map showed in (e) and (f). (e) Contour map of  $R_a$  factor for Pd 3d emission as function of Cu concentration in the first and second layer. (f) Same for Cu 3p emission.

three models could be simulated with a random alloy of the form  $\text{Cu}_x\text{Pd}_{(1-x)}/\text{Cu}_y\text{Pd}_{(1-y)}$ , where  $x$  and  $y$  are the Cu concentrations in the first and second layers, respectively. In Figs. 3(e) and 3(f), we present a contour map of the  $R_a$  factor as a function of the concentration of Cu in the first two layers for Pd 3d emitters and Cu 3p emitters, respectively. In order to initiate the simulation, we assumed the same number of atoms, Debye temperature, and inner potential as those used for Pd(111); initial structural parameters such as the inter-layer distances, were those of bulk terminated Pd(111). Using only the Cu 3p emitter data [Fig. 3(f)], we found a concentration of 85% of Cu in the first layer, but the results for the second layer were not conclusive. This was expected since the Cu 3p electrons are emitted almost in the forward scattering regime, and thus are not very sensitive to the concentration in the second layer. However, by combining the results of Cu 3p emitter with those considering the Pd 3d

electrons [Fig. 3(e)], it was possible to determine concentrations of 85 and 30 % of Cu in the first and second layers, respectively. We verified the applicability of other possible models (including, for example, Cu in the third layer), but in all cases the resulting  $R$  factor values increased. This was expected since no strong diffraction peaks were experimentally observed at polar angles around  $20^\circ$  in the Cu  $3p$  diffraction pattern, which are related to emitters in the most internal layers.

We should point out that our results for the concentrations in the first two layers for 1 ML of Cu on Pd(111) and those for 1 ML of Pd on Cu(111),<sup>13</sup> both annealed to 600 K, are basically the same. These results are especially significant within the context of the deposition of 3 ML of Cu on Pd(111) discussed in the next section.

Fixing the concentration of Cu in 85 and 30 %, respectively, in the first and second layers, the structural parameters were optimized. By using a grid search method and  $R$  factor analysis, we determined that the first interlayer distance contracted by  $0.5 \pm 0.8\%$  related to the bulk. Due the large error bar we assume bulk termination for the first interlayer distance. We should point out that, for the second interlayer distance, the search results using Pd and Cu emitters indicate a large contraction of  $7 \pm 2.5\%$ . However, in our model, the Cu concentration is significant only in the first and second layers, which makes the determination of the second interlayer distance very dependent on the back scattering signal. Since the photoelectron signal for Cu  $3p$  was mainly in the forward scattering regime, our result for the second interlayer spacing is, therefore, more imprecise.

#### D. Approximately 3 ML of Cu on Pd(111) annealed at 800 K

In many binary systems where the segregation energy is positive, the deposited metal is expected to diffuse into the bulk. Depending on the magnitude of this energy, however, under certain conditions the deposited metal can be trapped in the second layer with a capping layer of the substrate material.<sup>7,11,15,29,30</sup> Depending on the substrate temperature in the case of miscible metals, such as Cu and Pd, the deposited metal can alloy and evolve from a random to an ordered phase. Theoretical studies<sup>27</sup> show that, for the close packed fcc surface metals,  $c(2 \times 2)$  and  $(\sqrt{3} \times \sqrt{3})R30^\circ$  ordered phases are the most stable. In fact the Pd-Cu bonds are stronger than the Pd-Pd or Cu-Cu bonds, and apparently the exclusion of Pd-Pd nearest neighbors decreases the total energy of this system,<sup>28</sup> which in principle could be favoring  $c(2 \times 2)$  or  $(\sqrt{3} \times \sqrt{3})R30^\circ$  for the  $\langle 111 \rangle$  surface. This effect does not necessarily occur over a long-range because of the competition between the short-range interaction energies and entropy effects.<sup>7</sup>

Considering the similarity of the results of the previous section with those for Pd on Cu(111),<sup>13</sup> it would appear that, for a 1 ML deposition, the concentrations in the first two layers are independent of the substrate when the sample is annealed to 600 K. It seems likely that there is a barrier to the diffusion of Cu and Pd further than the second layer into Pd(111) and Cu(111) at 600 K, respectively. In view of these results, an interesting question regards the possibility of a

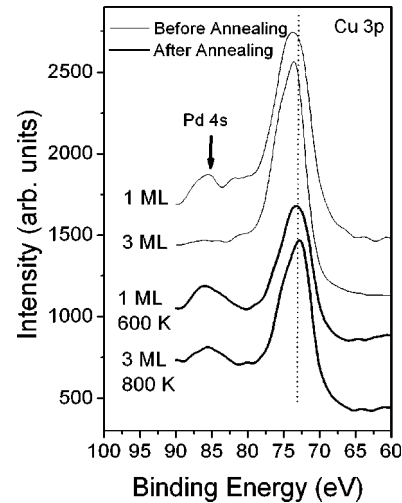


FIG. 4. XPS spectra for Cu  $3p$  for 1 and 3 ML of Cu on Pd(111) before (gray curves) and after annealing (black curves).

transition from a random phase to an ordered phase with increasing annealing temperature and also the stability of the barrier for Cu diffusion at higher temperatures.

To verify these point, the equivalent of 3 ML of Cu was deposited at 0.1 ML/min on to a clean Pd(111) surface with the substrate at room temperature and then annealed at 800 K (the temperature for the random to ordered phase transition in bulk PdCu alloys<sup>31,32</sup>) for 10 min and slowly cooled back to room temperature (approximately 30 min). The LEED pattern showed a sharp  $p(1 \times 1)$  structure with no evidence of ordered reconstruction. XPS indicated that the film was free of any kind of contamination.

Figure 4 shows the XPS spectra for the 1 and 3 ML films before and after annealing. Before annealing the Cu  $3p$  lines do not present chemical shifts, which agrees with the absence of alloying. After annealing the 1 ML film at 600 K and the 3 ML at 800 K, the Cu  $3p$  line shows a  $-0.6 \pm 0.1$  eV shift in the former case and a  $-0.8 \pm 0.1$  eV shift in the latter.

The PED raw data sets for the 3 ML film for Pd  $3d$  [Fig. 5(a)] and Cu  $3p$  [Fig. 5(b)] emitters were produced with photons of 700 eV (the same as that used in Ref. 13). Using the same methodology as in the previous section, a concentration search for the first and second layers was performed and the results are presented for Pd  $3d$  and Cu  $3p$  in Figs. 5(e) and 5(f), respectively. For both emitters, the results indicate a high concentration of Cu in the first layer, larger than 90% and a well defined minimum for the concentration of 75% of Cu on the second layer, a conclusion extracted mainly from the Pd emitter data. Simulations with Cu in the third layer produced higher  $R$  factors. This is expected from the experimental Cu  $3p$  PED pattern; since Cu emitters present in the third layer would produce three intense peaks in the azimuthal curve for polar angle  $\theta$  around  $20^\circ$ , but none were observed.

These observations might indicate a system with a capping layer of Cu of the type Cu/Cu<sub>75</sub>Pd<sub>25</sub>/Pd(111), but the simulation for this case resulted in an  $R_a$  factor for the Pd emitters of 0.6, which is much higher than for the case of Pd in the first layer, so that, even though the  $R_a$  factor for Cu  $3p$

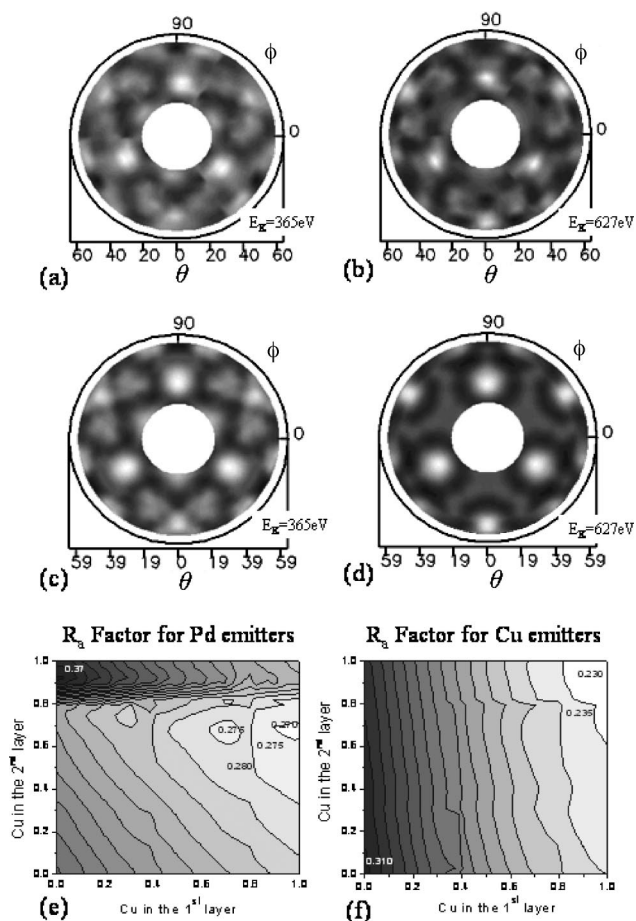


FIG. 5. Layer-by-layer determination of the surface alloy concentration and theory-experiment comparisons for PED data sets for 3 ML of Cu on Pd(111) annealed at 800 K and excited with photons of 700 eV. (a) Experimental raw data for Pd 3d emission; (b) experimental raw data for Cu 3p emission; (c) and (d) correspond to optimized PED theoretical simulations respectively for Pd 3d emission and Cu 3p emission considering a PdCu random alloy in the first and second layers with the concentrations found by the  $R_a$  factor contours map showed in (e) and (f). (e) Contour map of  $R_a$  factor for Pd 3d emission as function of Cu concentration in the first and second layer. (f) Same for Cu 3p emission.

emitters was  $0.230 \pm 0.005$ , consideration of all the data indicates that a capping layer of Cu seems improbable. These results indicate the presence of a small amount of Pd in the first layer, probably less than 10%, this agrees with theoretical studies that point to a strong segregation of Cu to the surface in the PdCu alloys.<sup>6</sup>

The 75% concentration of Cu in the second layer corresponds exactly to that necessary to form a  $(2 \times 2)$ -Cu<sub>3</sub>Pd ordered phase. Notwithstanding the absence of any sign of ordering in the LEED patterns, we performed simulations with the first layer a random phase with 95% Cu and 5% Pd treated using the ATA approach and the second layer an ordered  $(2 \times 2)$ -Cu<sub>3</sub>Pd phase over bulk Pd(111). The  $R_a$  factors were slightly smaller for an ordered second layer rather than a random one: for the Cu 3p emitters,  $R_a = 0.204 \pm 0.005$  for an ordered second layer and  $0.235 \pm 0.005$  for a random second layer; for the Pd 3d emitters,  $R_a = 0.262 \pm 0.005$  for both

cases. Another, independent, way to determine the correct model is by using the  $R_b$  factor that is also sensitive to the intensities and consequently to the scattering amplitudes described by the distribution of the atomic scattering potentials around the emitters. If a model with an ordered distribution correctly places the species around the emitters, the corresponding description of the intensities should be better than that produced by the ATA approach, which describes the scattering properties of all atoms in the layer just by an average of the atomic scattering factors weighted by the concentrations.<sup>22</sup> The  $R_b$  factor was  $0.204 \pm 0.005$  for the random second layer and  $0.052 \pm 0.005$  for the ordered one, a significant improvement. It is important to note that, to describe correctly the intensities in a PED experiment, it is necessary to know not only the atomic positions and concentrations but also the phase shifts, photoemission transition probabilities, attenuation due to the mean free path and vibration dependencies, which, except for the very simplest cases, are not known, so that approximations and estimates are used, which could affect the validity of the results. The fact that LEED did not show ordering in the second layer could be due to its lack of sensitivity to short-range order or to smaller energy of the LEED electrons relative to the photoelectrons used in the PED measurements.

The interlayer distances were independent of which model (random or ordered) was used for the second layer and indicated an expansion of  $2.0 \pm 0.8\%$  in the first interlayer distance. For the same argument explained before, the Cu 3p signal is little sensitive to the second interlayer distance. By fixing the first interlayer distance found before, we optimized the second interlayer distance in order to minimize the  $R$  factors for Pd 3d PED, which indicate a minimum for an expansion of  $1.3 \pm 0.8\%$  in the second interlayer distance. The in-plane interatomic distances were the same as for bulk Pd(111). From the PED analysis of a 1 ML of Pd on Cu(111),<sup>13</sup> an expansion of +5.0% in the first interlayer distance was observed,<sup>13</sup> which is about three times larger than the corresponding value found here for Cu on Pd(111). The reason for this difference might be due to the difference in the atomic radii between Pd and Cu. Since Pd is bigger than Cu, it is reasonable to expect a larger surface expansion on the Pd on Cu(111) system in order to accommodate the Pd atoms. Here, the deposited Cu atom is smaller than the Pd atoms of the substrate, resulting in a small change on the topmost interlayer distance.

#### IV. CONCLUSIONS

Cu on Pd(111) is complementary to Pd on Cu(111) and, speaking generally, forms a surface random alloy, but with some important differences. With the substrate at room temperature, Cu grows on Pd(111) layer-by-layer and does not alloy with the substrate. On the other hand, Pd on Cu(111), has a more complicated growth mode, with Pd alloying to Cu in the submonolayer regime even at room temperature.

In this paper, we studied the growth characteristics of Cu deposited on Pd(111). We present also the results of the first PED study of clean Pd(111). The first interlayer distance is in agreement with those derived from LEED (Ref. 23) and from a theoretical investigations.<sup>25</sup>

For 1 ML of Cu on Pd(111) alloy formation starts around 450 K, and we conclude that Cu diffuses into the Pd (111) bulk at 600 K up to the second layer, forming a random alloy with the same concentrations as found for Pd on Cu(111).<sup>13</sup> There appears to be a barrier for diffusion of Cu into Pd(111) and of Pd into Cu(111) beyond the second layer: we should note that, at the present time, we cannot confirm the existence of the suggested diffusion barrier.

For 3 ML of Cu evaporated onto Pd(111) and annealed to 800 K we also have no evidence of Cu diffusing beyond the second layer, supporting the suggestion of a diffusion barrier. Additionally, Pd remains in the first layer only at very low concentrations, that is in agreement with the expected strong Cu segregation to the surface in the Pd/Cu system. We should note that the Cu concentration in the second layer derived from our analysis is identical to that needed to form a (2×2)-Cu<sub>3</sub>Pd. Careful analysis of the *R* factors for indicates the possibility of short-range ordering in the second

layer, but further experiments and theoretical work are needed to substantiate this conclusion.

Structural parameters for 3 ML of Cu deposited indicate are much smaller than for Pd/Cu(111). For Cu/Pd(111), the first two interlayer distance seems to expand around 2% for the first and 1.3% for the second. Those for Pd/Cu(111) seem to correspond to a first layer expansion of 5% and a second layer contraction of around 2%. These differences are consistent with considerations based on the relative sizes of the Cu and Pd atoms.

#### ACKNOWLEDGMENTS

The authors would like to thank A. R. B. de Castro, P. T. Fonseca and the IUUV staff for helping during the beam time at LNLS. FAPESP, CNPq, and LNLS of Brazil supported this work. A. S. would like to thank CAPES for financial support. Part of the PED calculation was performed on the PC Clusters at Universidade Federal da Bahia.

\*E-mail address: abner@lnls.br and asiervo@ifi.unicamp.br

Present address: Universität Dortmund, Experimentelle Physik I, Otto-Hahn-Straße 4, D-44221 Dortmund, Germany.

<sup>1</sup>J. A. Rodriguez, Surf. Sci. Rep. **24**, 223 (1996).

<sup>2</sup>F. Besenbacher, I. Chorkendorff, B. S. Clausen, B. Hammer, A. M. Molenbroek, J. K. Nørskov, and I. Stensgaard, Science **279**, 1913 (1998).

<sup>3</sup>A. P. Villar and L. D. Calvet, in *Pearson's Handbook of Crystallographic Data for Intermetallic Phases* (ASM International, Materials Park, OH, 1991).

<sup>4</sup>S. K. Bose, J. Kudrnovský, O. Jepsen, and O. K. Andersen, Phys. Rev. B **45**, 8272 (1992), and references therein.

<sup>5</sup>J. E. Garces, G. H. Bozzolo, P. Abel, and H. O. Mosca, Appl. Surf. Sci. **167**, 18 (2000); J. E. Garces, H. O. Mosca, and G. H. Bozzolo, Surf. Sci. **459**, 365 (2000).

<sup>6</sup>A. V. Ruban, H. L. Skriver, and J. K. Nørskov, Phys. Rev. B **59**, 15 990 (1999).

<sup>7</sup>C. Creemers, P. Deurinck, S. Helfensteyn, and J. Luyten, Appl. Surf. Sci. **219**, 11 (2003).

<sup>8</sup>C. Barnes and M. Gleeson, Surf. Sci. **319**, 157 (1994).

<sup>9</sup>F. Illas, N. López, J. M. Ricart, A. Clotet, J. C. Conesa, and M. Fernández-García, J. Phys. Chem. B **102**, 8017 (1998).

<sup>10</sup>G. Liu, T. P. St. Clair, and D. W. Goodman, J. Phys. Chem. B **103**, 8578 (1999).

<sup>11</sup>A. Christensen, A. V. Ruban, and H. L. Skriver, Surf. Sci. **383**, 235 (1997).

<sup>12</sup>A. Bach Aaen, E. Laegsgaard, A. V. Ruban, and I. Stensgaard, Surf. Sci. **408**, 43 (1998).

<sup>13</sup>A. de Siervo, E. A. Soares, R. Landers, T. A. Fazan, J. Morais, and G. G. Kleiman, Surf. Sci. **504**, 215 (2002).

<sup>14</sup>P. W. Murray, I. Stensgaard, E. Laegsgaard, and F. Besenbacher, Phys. Rev. B **52**, R14 404 (1995).

<sup>15</sup>P. W. Murray, S. Thorshaug, I. Stensgaard, F. Besenbacher, E. Laegsgaard, A. V. Ruban, K. W. Jacobsen, G. Kopidakis, and H. L. Skriver, Phys. Rev. B **55**, 1380 (1997).

<sup>16</sup>R. Paniago, A. de Siervo, E. A. Soares, H.-D. Pfannes, and R. Landers, Surf. Sci. **560**, 27 (2004).

<sup>17</sup>E. Hahn, E. Kampshoff, N. Wälchli, and K. Kern, Phys. Rev. Lett. **74**, 1803 (1995).

<sup>18</sup>E. Hahn, E. Kampshoff, A. Frincke, J.-P. Bucher, and K. Kern, Surf. Sci. **319**, 277 (1994).

<sup>19</sup>B. Oral and R. W. Vook, J. Vac. Sci. Technol. A **8**, 3048 (1990).

<sup>20</sup>A. de Siervo, R. Paniago, E. A. Soares, H.-D. Pfannes, R. Landers, and G. G. Kleiman, Surf. Sci. **575**, 217 (2005).

<sup>21</sup>Y. Chen and M. A. Van Hove, Multiple Scattering Calculation Diffraction Package, <http://electron.lbl.gov/mscdpackage/>

<sup>22</sup>E. A. Soares, A. de Siervo, R. Landers, and G. G. Kleiman, Surf. Sci. **497**, 205 (2002).

<sup>23</sup>H. Ohtani, M. A. Van Hove, and G. A. Samorjai, Surf. Sci. **187**, 372 (1987).

<sup>24</sup>Y. Kuk, L. C. Feldman, and P. J. Silverman, Phys. Rev. Lett. **50**, 511 (1983).

<sup>25</sup>Ch. Konvicka, Y. Jeanvoine, E. Lundgren, G. Kresse, M. Schmid, J. Hafner, and P. Varga, Surf. Sci. **463**, 199 (2000).

<sup>26</sup>A. Canzian, H. O. Mosca, and G. Bozzolo, Surf. Sci. **551**, 9 (2004).

<sup>27</sup>Y. Teraoka, Surf. Sci. **235**, 249 (1990).

<sup>28</sup>F. R. DeBoer, R. Boom, W. C. M. Mattens, A. R. Miedema, and A. K. Niessen, *Cohesion in Metals: Transition Metal Alloys*, edited by F. R. DeBoer and D. G. Pettifor (Elsevier, Amsterdam, 1998).

<sup>29</sup>J. L. Rousset, J. C. Bertolini, and P. Miegge, Phys. Rev. B **53**, 4947 (1996).

<sup>30</sup>J. P. Reilly, C. J. Barnes, N. P. Price, R. A. Bennett, S. Poulston, P. Stone, and M. Bowker, J. Phys. Chem. B **103**, 6521 (1999).

<sup>31</sup>R. V. Chepulkii, J. B. Staunton, Ezio Bruno, B. Ginatempo, and D. D. Johnson, Phys. Rev. B **65**, 064201 (2002).

<sup>32</sup>M. Rodewald, K. Rodewald, P. De Meulenaere, and G. Van Tendeloo, Phys. Rev. B **55**, 14 173 (1997).